Journal of Molecular and Cellular Cardiology 45 (2008) 742–753

Contents lists available at ScienceDirect

Journal of Molecular and Cellular Cardiology

journal homepage: www.elsevier.com/locate/yjmcc

Original article

# Upregulation of matrix metalloproteinase-9 and tissue inhibitors of metalloproteinases in rapid atrial pacing-induced atrial fibrillation

Chien-Lung Chen [a], Shoei K. Stephen Huang [b], Jiunn-Lee Lin [c], Ling-Ping Lai [c], Shao-Chuan Lai [a], Chia-Wei Liu [a], Wen-Chi Chen [a], Cheng-Hao Wen [a], Chih-Sheng Lin [a,*]

[a] Department of Biological Science and Technology, National Chiao Tung University, No. 75 Po-Ai Street, Hsinchu 30068, Taiwan
[b] Division of Cardiology, Scott and White Clinic, Texas A&M University College of Medicine, Temple, Texas, USA
[c] Division of Cardiology, Department of Internal Medicine, National Taiwan University Hospital, Taipei, Taiwan

ARTICLE INFO

*Article history:*
Received 23 January 2008
Received in revised form 27 June 2008
Accepted 3 July 2008
Available online 23 July 2008

*Keywords:*
Atrial fibrillation
Extracellular matrix
Gelatinases
Matrix metalloproteinases
MMP-9
Tissue inhibitors of metalloproteinases

ABSTRACT

Remodeling of atrial extracellular matrix (ECM) in atrial fibrillation (AF) involves changes in the expression of matrix metalloproteinases (MMPs) and tissue inhibitors of MMPs (TIMPs). The contributions of MMPs and TIMPs to the pathogenesis of AF development have not been clearly defined. This study evaluated the *in situ* activity and expression of gelatinases (MMP-2 and MMP-9) and their relationship with TIMP-1 or TIMP-3 in atria undergoing rapid atrial pacing for the induction of AF (4 weeks' pacing followed by 2 weeks of maintained AF) in pigs. In AF atria, *in situ* gelatinase activity was mainly localized in the interstitium of atrial myocardium, and was significantly larger than that of sinus rhythm control (i.e., sham control). The significant increase of MMP-9 in its pro-form and mRNA level, but not MMP-2, was shown to be responsible for the increased gelatinase activity in atria with AF. The inhibitory activities of glycosylated TIMP-1 and TIMP-3, but not TIMP-2, in AF tissues were markedly elevated and also localized in the atrial interstitium. TIMP-1 was found to be mostly colocalized with gelatinase activity over the AF tissues, implying the coexistence of gelatinase activity and TIMP-1, but TIMP-3 appeared only partially colocalized and discontinued the gelatinase activity surrounding the cardiomyocytes. TIMP-1 and TIMP-3 may play differential roles in the inhibition of gelatinase activity *in vivo*. Together with the survey of several MMPs transcripts and the level of transforming growth factor-β1 (TGF-β1), we proposed that the increased activity of gelatinase (i.e., MMP-9), TIMP-1 and TIMP-3 and their interaction may contribute to atrial ECM remodeling of AF.



## 1. Introduction

Atrial fibrillation (AF) is the commonest arrhythmia seen in clinical practice. The longer the duration of AF, the more persistent AF becomes because of atrial electrical and structural remodeling. Recent findings suggest that AF itself causes changes in the function and structure of the atrium, providing a possible explanation for the progressive nature of this arrhythmia [1,2]. Structural abnormalities in AF are associated with changes in the components of the extracellular matrix (ECM) [3,4], which may be involved in progressive remodeling of the atrium, thereby increasing vulnerability to AF. Although electrical, contractile and structural remodeling has been characterized during AF, the structural remodeling of atrium is considered the major contributor to AF persistence [5]. The ECM provides supportive scaffolding for cardiomyocytes, maintains the structural integrity of cardiac tissue, and is necessary for electrical conduction via cardiomyocytes. Therefore, changes in the expression and activity of proteolytic enzymes and their inhibitors that regulate ECM components in the atrium may play an important role in the development of sustained AF [4,6]. Accordingly, the detailed mechanism of ECM-regulating enzymes and factors relating to structural remodeling in AF progression must be elucidated.

Matrix metalloproteinases (MMPs) are important enzymes involved in the normal processes associated with turnover of connective tissue, such as morphogenesis, uterine involution, bone resorption, and wound repair [7–10]. MMPs can break down ECM with a broad range of substrate specificities and can cause tissue remodeling [10,11]. ECM degradation by MMPs is associated with the pathogenesis of cardiovascular diseases, including atherosclerosis, restenosis, dilated cardiomyopathy, myocardial infarction, and heart failure (HF) [12–14]. Cardiomyocytes can synthesize and release MMPs, in particular MMP-2 (gelatinase A) and MMP-9 (gelatinase B), which participate in the ventricular remodeling process [15,16]. In addition, under pathological conditions with changed MMP activities, alterations of the levels of endogenous tissue inhibitors of metalloproteinases (TIMPs) are also considered important because they directly inhibit MMP activity [10,17]. The studies cited above indicate

* Corresponding author. Tel.: +886 3 5131338; fax: +886 3 5729288.
*E-mail address:* lincs@mail.nctu.edu.tw (C.-S. Lin).

0022-2828/$ – see front matter © 2008 Elsevier Inc. All rights reserved.
doi:10.1016/j.yjmcc.2008.07.007

that the interplay between MMPs and TIMPs have a regulatory role in myocardial remodeling.

In our recent studies [18–20], myocardial remodeling involving an increased level of interstitial fibrosis in the atrium in rapid atrial pacing (RAP)-induced AF model was observed. The regulation of MMPs and TIMPs involved in the structural remodeling of atria with RAP-induced AF is not well understood. In the present study, the results support our hypothesis that changes in the expression of atrial MMPs and TIMPs may be differentially evolved in RAP-induced AF, and may play a part in atrial remodeling.

## 2. Materials and methods

### 2.1. Atrial tissues with AF

The experimental protocol conformed to the Guide for the Care and Use of Laboratory Animals published by National Institutes of Health (NIH Publication No. 85-23, revised 1996) and was approved by the animal welfare committees of National Chiao Tung University and National Taiwan University. Pigs were provided by the Animal Technology Institute Taiwan and housed in their animal facility.

Frozen atrial tissues from 15 adult Yorkshire–Landrace pigs, including 9 AF and 6 sham control (sinus rhythm; SR) tissues, were used in the present study. We have previously characterized these tissues with respect to the pathological changes of myocardial fibrosis and the gene expression profile associated with the RAP-induced AF [18,19]. The RAP-induced AF pig model was established by Lin et al. [21]. In brief, each pig was transvenously implanted with a high-speed atrial pacemaker (Itrel-III; Medtronic Inc., Minneapolis, MN, USA) programmed to produce a pacing rate of 400–600 beats per min in the right atrial appendage for four weeks in the AF group. After continuous pacing for four weeks, the atrial pacemaker was turned off, and the pigs remained in sustained AF. Pigs were sacrificed two weeks after the pacemaker was turned off. The treatment period was therefore six weeks: rapid pacing for four weeks and AF without pacing for two weeks. As in our previous study [19,21], permanent AF in these pigs was confirmed through Holter monitoring. In the sham SR group, the pacemaker was turned off for the entire six weeks after implantation. During the period of atrial pacing, digoxin (0.25 mg per day, p.o.) was given daily to control heart rate to minimize the possibility of developing severe congestive heart failure (HF). Pigs of the SR control group were also given digoxin (0.25 mg per day, p.o.). Pigs were examined by transthoracic echocardiography before sacrifice. There was no significant difference in heart rate between SR (78±5 beats per min) and RAP-induced AF (83±8 beats per min) groups [19].

### 2.2. Protein isolation and electrophoresis

Frozen atrial tissues (200 mg) were homogenized in 1 ml of ice-cold lysis buffer containing 20 mM Tris–HCl, pH 7.6, 1 mM dithiothreitol, 200 mM sucrose, 1 mM EDTA, 0.1 mM sodium orthovanadate, 10 mM sodium fluoride, 0.5 mM phenylmethylsulfonyl fluoride (PMSF) and 1% (v/v) Triton X-100. Homogenates were centrifuged at 10,000 ×*g* for 30 min at 4 °C. Supernatants were collected, and protein concentration determined by Bio-Rad protein assay kit (Bio-Rad Laboratories, Hercules, CA, USA) with bovine serum albumin as a standard. Equal amounts of total protein (20 μg/lane) were separated by 10% sodium dodecyl sulfate polyacrylamide gel electrophoresis (SDS-PAGE).

### 2.3. In situ zymography

Localization of gelatinase activities in sections of atrial tissue was done by *in situ* zymography as described in [22] with minor modifications. In brief, fresh frozen sections (6 μm) were mounted onto slides with 0.05 mg/ml DQ-gelatin in 1% (w/v) low-gelling temperature agarose (Sigma, St. Louis, MO) in phosphate-buffered saline (PBS) containing 0.5 μg/ml propidium iodide (PI) to counterstain nuclei and 50 mM phenylmethylsulfonylfluoride (PMSF). PMSF in the mixture ensured that increased fluorescence was not due to a serine protease [23]. After gelling of the agar at 4 °C, incubation was done at 37 °C for 4 h. Gelatinase activity resulted in the loss of quenching and was visualized by a fluorescent signal. As a control, inhibition of MMP gelatinase activity was carried out by preincubation of cryostat sections in PBS containing 20 mM EDTA for 1 h at room temperature, followed by DQ-gelatin incubation in 20 mM EDTA. A microscope (Olympus, Melville, NY, USA) equipped with a mercury lamp and epifluorescence optics was used to visualize fluorescence. The area of green fluorescence in digital images was quantified by Image-Pro Plus 6.0 software (Media Cybernetics, Silver Spring, MD, USA).

### 2.4. Gelatin zymography

Zymography was done using gelatin-containing gels as described by Stawowy et al. [24]. Briefly, 20 μg of non-denatured atrial homogenate was mixed with 2′ zymography sample buffer (0.125 M Tris–HCl, pH 6.8, 20% (v/v) glycerol, 4% (w/v) SDS, and 0.005% bromophenol blue) and incubated for 10 min at room temperature, and loaded into each lane of a SDS-PAGE (10%) containing 0.1 mg/ml gelatin (Sigma). After electrophoresis, the gel was washed twice for 30 min in zymogram renaturing buffer (2.5% Triton X-100) with gentle agitation at room temperature to remove SDS, and then incubated at 37 °C overnight in reaction buffer (50 mM Tris–HCl, pH 7.4, 200 mM NaCl, and 5 mM $CaCl_2$). After staining with Coomassie brilliant blue, gelatinase activities were identified as clear zones against a blue background. Confirmation of gelatinase activity corresponding to the pro-form and active form of MMP-2 and MMP-9 was executed with *p*-aminophenylmercuric acetate (APMA; Sigma) treatment as described by Stetler-Stevenson et al. [25]. Pro-forms of MMP-9 and MMP-2 can be activated by APMA generating full active species. Briefly, atrial homogenates were incubated in APMA working buffer (1 mM APMA, 20 mM Tris–HCl, pH 7.5, 0.4 mM $CaCl_2$, and 0.02% Triton X-100) at 37 °C for 0–60 min and loaded onto gels as described above. Gelatinase activities in the gel slabs were quantified using ScionImage software (NIH, Bethesda, MD, USA), which quantifies the extent of lysis in bands containing gelatinase. A

**Table 1**
Primers for semi-quantitative RT-PCR

| Genes | Gene symbol/ accession no. | Forward primers (5′→3′) Reverse primers (5′→3′) | Product size (bp) |
|---|---|---|---|
| Matrix metalloproteinases-1 | MMP-1/ X54724 | GCC CAC AAA CCC CAC AAG CTT CCT CAA AAA CAG CAG CAT C | 342 |
| Matrix metalloproteinases-2 | MMP-2/ NM_214192 | ATA CCA AGA ACT TCC GCC CAG CCA GTC GGA TTT GAT | 695 |
| Matrix metalloproteinases-3 | MMP-3/ AF201725 | TGT GGA GTT CCT GAT GTT GGT TTT CCA GGT CCG TCA AAA GG | 263 |
| Matrix metalloproteinases-9 | MMP-9/ NM_174744 | GGC ACC ACC ACA ACA TCA GCG GTC GGC GTC GTA GTC | 452 |
| Matrix metalloproteinases-14 | MMP-14/ NM_214239 | CCT CAA CCC AGG ACC ACC TC GCA TCC AGA AGA GAG CAG CA | 385 |
| Tissue inhibitor of metalloproteinases-1 | TIMP-1/ NM_213857 | GCA ACT CCG ACC TTG TCA TC AGC GTA GGT CTT GGT GAA GC | 326 |
| Tissue inhibitor of metalloproteinases-2 | TIMP-2/ AF156030 | GTA GTG ATC AGG GCC AAA GC TTC TCT GTG ACC CAG TCC AT | 416 |
| Tissue inhibitor of metalloproteinases-3 | TIMP-3/ AF156031 | CGT GTC TAT GAT GGC AAG ATG CAG GCG TAG TGT TTG GAC TG | 233 |
| Glyceraldehyde-3-phosphate dehydrogenase | GAPDH/ AF017079 | ATGGTGAAGGTCGGAGTGAACGGA TGATGTTCTGGAGAGCCCCTCGG | 613 |

Primer sequences for each target gene were selected to minimize the formation of self-complementarity and hairpins using PRIMER3 software (available online at http://frodo.wi.mit.edu/primer3/input.htm).

MMP-2 positive control (Chemicon, Temecula, CA, USA) was loaded in each gel as a standard to normalize density values, and band intensities were expressed in arbitrary units.

### 2.5. Reverse gelatin zymography

The MMP-inhibitory activity of TIMPs was analyzed by reverse zymography as described [26] with slight modification. Samples containing 20 μg of atrial homogenate were mixed with an equal volume of 2′ zymography sample buffer, incubated for 10 min at room temperature, and then subjected to SDS-PAGE on a 12% gel prepared with 1 mg/ml gelatin and 0.1 mg/ml human MMP-2 (Chemicon). After electrophoresis, gels were washed twice in 100 ml of 2.5% Triton X-100 solution on a rotary shaker for 30 min, and followed by incubation in 100 ml of developing buffer (50 mM Tris, pH 7.5, 5 mM $CaCl_2$, and 1 mM $ZnCl_2$) at 37 °C for 48 h. Gels were stained with Coomassie brilliant blue followed by destaining. Because TIMP inhibits gelatinase activity, the migration of TIMP in the gel was visualized as dark blue bands on a lighter background. The relative intensities of TIMP were determined by densitometric analysis. Analysis of all samples by SDS-PAGE lacking the gelatin substrate was also performed to demonstrate no significant detectable protein staining corresponding to the TIMP bands determined in the presence of gelatin.

### 2.6. Semi-quantitative reverse transcription-polymerase chain reaction (RT-PCR)

Semi-quantitative RT-PCR was done according to our previous studies [20]. For cDNA synthesis, 3 μg RNA was supplemented in a total reaction volume of 20 μl with 1′ RT buffer, 0.5 mM dNTPs, 2.5 μM oligo-dT (Invitrogen, Carlsbad, CA, USA), 40 U/μl RNase inhibitor (Invitrogen), and 20 U/μl Superscript II™ reverse trascriptase (Invitrogen). After incubation at 50 °C for 60 min, the mixture was incubated at 70 °C for 15 min to denature the products. PCR primers for RT-PCR analysis are shown in Table 1. PCR reactions contained 2 μl cDNA, 1 μl each primer (10 μM), 5 μl 10′ PCR buffer, 2 μl 10 mM dNTPs, 1 μl 5 U/μl Taq polymerase (Violet Bioscience, Hsinchu, Taiwan) and 38 μl distilled water in a total volume of 50 μl. Thermal cycler (MiniCycler™; MJ Research, Waltham, MA, USA) condition was as follows: 1 cycle of 5 min at 94 °C, 26–38 cycles of denaturation at 94 °C for 30 s, annealing at 55 °C for 30 s, elongation at 72 °C for 45 s, and 1 cycle of 5 min at 72 °C. PCR products were visualized on 2% agarose

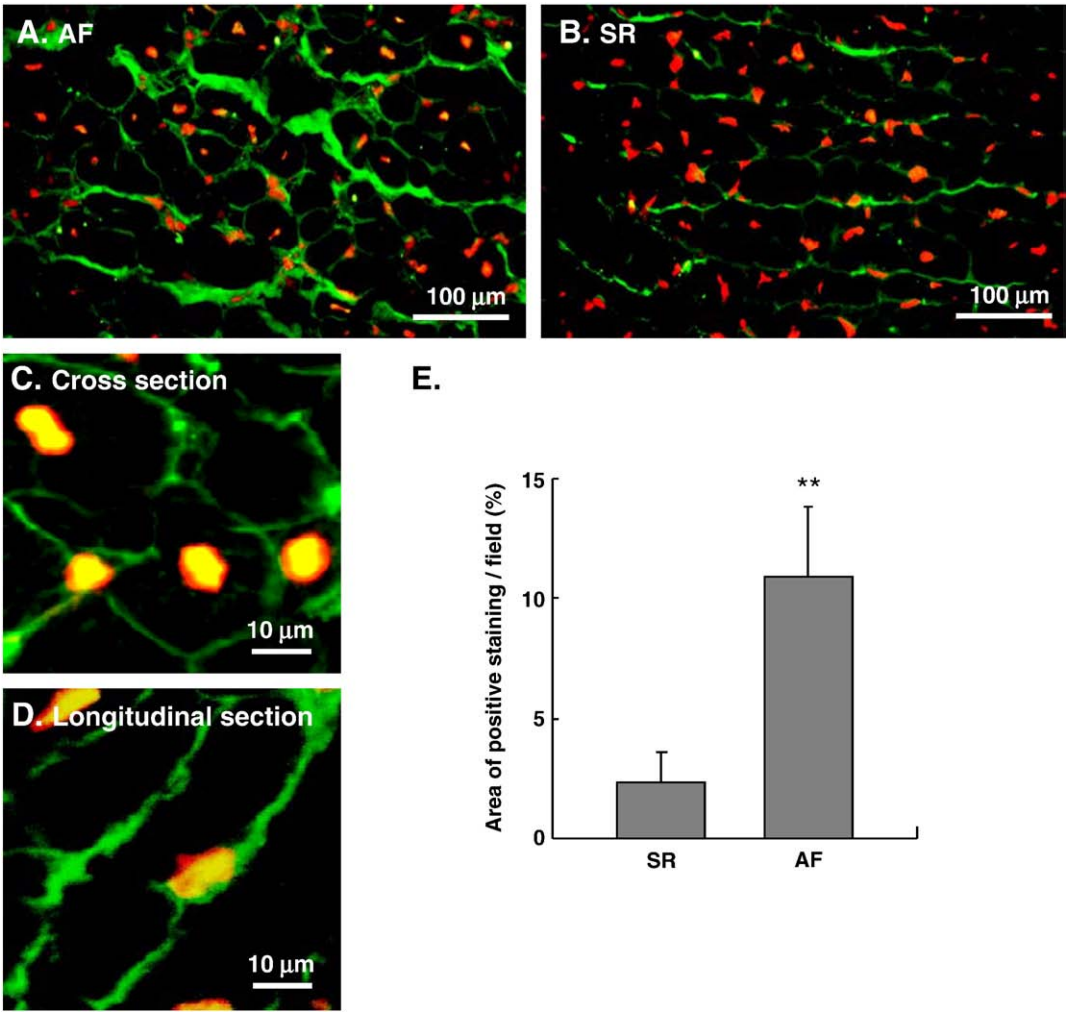


**Fig. 1.** Gelatinase activity (representing the activity of MMP-2 and MMP-9) in atria with AF and SR using *in situ* zymography. DQ-gelatin substrate and propidium iodide stain (nuclear stain; red fluorescence) were applied to the unfixed cryostat sections of atrial tissues. Increased green fluorescence, indicating gelatinase activity, which was caused by the breakdown DQ-gelatin, was localized at the atrial interstitium in the AF samples (A) as compared with SR samples (B). In AF tissues, the localization of green signal had a thicker fibrillar appearance in the interstitium of myocardium (A) and surrounding the cardiomyocytes (C and D). In SR tissues, there was only a fine network of gelatinase activity in the atrial interstitium (B) and only slight gelatinase activity was localized between the cardiomyocytes. Quantitative differences between the atrial tissues of SR ($n=6$) and AF ($n=9$) from the *in situ* zymography indicated a significant increase in gelatinolytic activity in the atrial tissues with AF (E). Each bar indicates mean±SD. $^{**}p<0.01$ *vs.* SR.

gels stained with ethidium bromide. The stained image was recorded by an image analyzer (Kodak DC290 Digital camera System™; Eastman Kodak, Rochester, NY, USA) and the band intensity was quantified using densitometric analysis by ScionImage software (NIH). Relative expression of mRNA of MMPs and TIMPs were calculated as ratios to expression of glyceraldehyde-3-phophate dehydrogenase (GAPDH).

### 2.7. Immunohistochemistry and immunofluorescence

Immunostaining studies were done according to our previous report [18]. Briefly, 6 μm atrial tissue sections were rehydrated and blocked with 3% hydrogen peroxide followed by incubation in 10% (v/v) normal goat serum (Santa Cruz Biotechnology, Santa Cruz, CA, USA). Tissue sections were incubated at 4 °C overnight with an antibody specific for TIMP-1 (Chemicon) or TIMP-3 (Santa Cruz Biotechnology) in Tris-buffered saline (10 mM Tris–HCl, pH 8.0, and 150 mM NaCl), followed by incubation with biotinylated secondary antibody (Vectastain Elite ABC kit; Vector Laboratory, Burlingame, CA, USA) for immunohistochemistry or secondary antibody conjugated with rhodamine (Chemicon) for immunofluorescence. Streptavidin-horseradish peroxidase (HRP) was used to develop antibody signals according to the manufacturer's instructions (Vector Laboratory). Nuclei were counterstained with hematoxylin. For the double-immunofluorescence staining experiments, cardiac fibroblasts and cardiomyocytes in the AF atria were identified by immunostaining with vimentin-specific antibody (DakoCytomation, Copenhagen, Denmark) and cardiac troponin T-specific antibody (Abcam, Cambridge, UK), respectively. Secondary antibody conjugated with FITC (Chemicon) was used to visualize the vimentin and troponin T signal, and nuclei were counterstained by 4′,6-diamidino-2-phenylindole (DAPI). To control for nonspecific signal, a duplicate sample was prepared as above, but omitting primary antibody. Each digital image was analyzed by Image-Pro Plus 6.0 software.

### 2.8. Dual labeling fluorescence and colocalization analysis

Dual fluorescent label was carried out with the combination of *in situ* zymography with minor modifications and immunofluorescent staining. Briefly, unfixed cryostat sections (6 μm) on poly-L-lysine-coated glass slides were incubated with 0.05 mg/ml DQ-gelatin in PBS containing 50 mM PMSF at 37 °C for 4 h in a humid chamber. After washing and fixing the slides in 1% paraformaldehyde, immunofluorescent staining was done as described above. Fluorescence labeling was done with a confocal laser scanning biological microscope (Fluoview FV500, Olympus, Tokyo, Japan). To prevent cross-talk between fluorescent labels, images were captured by sequential scanning and exchanging excitation/emission filters for each fluorogenic substrate. To determine the levels of gelatinase activity coexisting within the locations of TIMPs in AF atrium, the mean percentage of overlapping areas between gelatinase activity and the inhibitors (TIMP-1 or TIMP-3) *vs.* the areas labeled for each inhibitor was analyzed using Image-Pro Plus 6.0 software and reported as percentage colocalization.

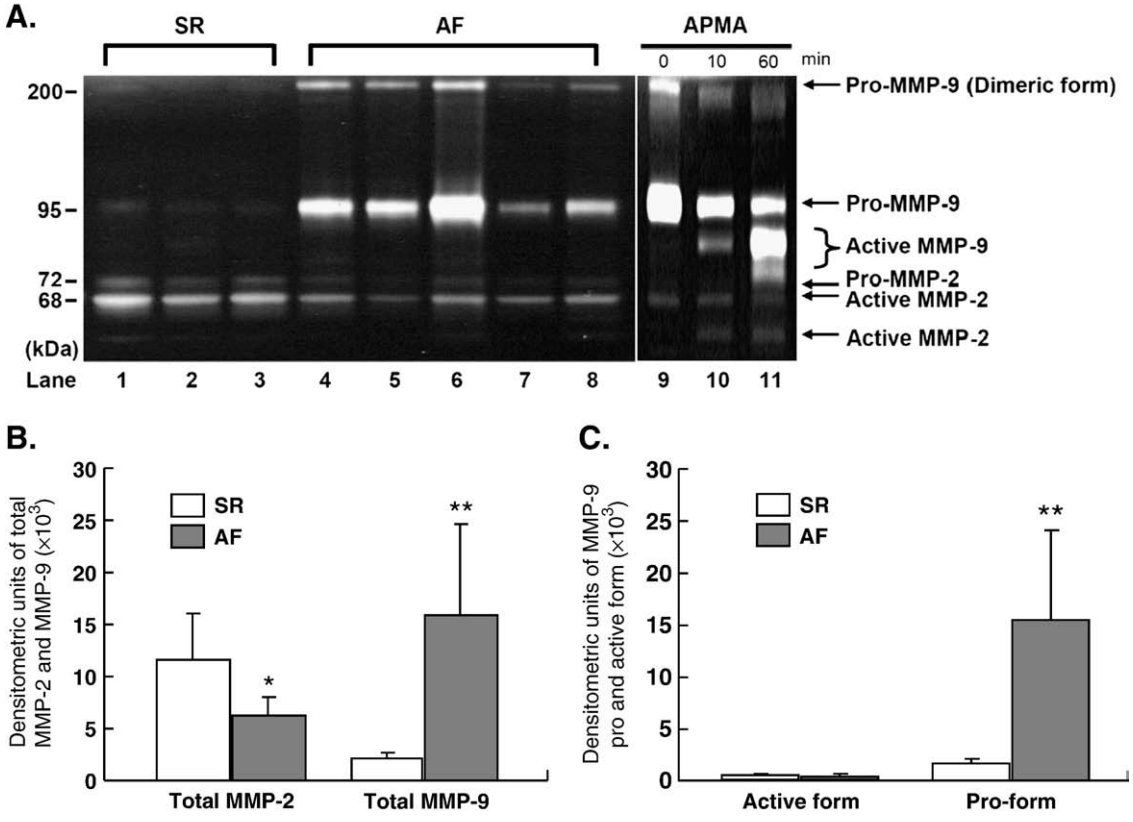


**Fig. 2.** Activity of MMP-2 and MMP-9 in atria with AF and SR. (A) Representative analysis of atrial homogenates (20 μg of total protein per sample) subjected to SDS-PAGE followed by in-gel zymography was shown. A comparison of predominant gelatinase activities from the AF and SR samples representing dimeric proMMP-9 (~220 kDa), proMMP-9 (95 kDa), proMMP-2 (72 kDa) and activated MMP-2 (68 kDa) is shown in lanes 1–8. Confirmation of migration of the latent and active MMP-2 and MMP-9 forms was done by treating homogenate of AF tissue with APMA followed by SDS-PAGE and in-gel zymography. The result revealed that the gelatinolytic enzymes in AF tissue were primarily comprised of pro-form MMP-9 and were activated by APMA (A; lanes 9–11). Molecular mass markers are indicated at the left. (B) Quantification of gelatinase activity was achieved by computer-assisted image analysis of zymographic gels. The increase of MMP-9 activity in AF samples ($n=9$) when compared with SR samples ($n=6$) was statistically significant. In contrast, there was a significant decrease in MMP-2 activity in AF samples as compared with SR samples. (C) Gelatinase activity of the pro-form MMP-9 was significantly upregulated in AF samples, but the active form of MMP-9 between the AF and SR groups was similar. Each bar indicates mean±SD. *$p<0.05$; **$p<0.01$ *vs.* SR.

### 2.9. Western blot analysis

Western blotting was carried out to determine the protein levels of transforming growth factor-β1 (TGF-β1) in atrial AF and SR tissues. Equal amounts of atrial homogenate (20 μg/lane) were separated on 12% polyacrylamide gels by SDS-PAGE, and transferred onto PVDF membranes (Millipore, Bedford, MA, USA) at 50 mA for 90 min in a semi-dry transfer cell (Bio-Rad). Membranes were blocked for 60 min in TBS (10 mM Tris–HCl, 0.15 M NaCl, pH 7.4) containing 5% non-fat dry milk with gentle agitation. Following three washes with TBS containing 0.1% (v/v) Tween-20 for 5 min, the membrane was incubated with anti-human TGF-β1 (1:3000) or anti-human β-tubulin (1:3000; antibodies were from Santa Cruz Biotechnology), and detected using HRP-conjugated secondary antibody and ECL western blotting detection reagents (Amersham Pharmacia Biotech, Little Chalfont, UK). The average densitometric analysis of the bands was carried out by Scion image software (NIH). Relative protein expression of TGF-β1 was normalized to β-tubulin expression.

### 2.10. Data analysis

For quantification of the *in situ* zymography, immunofluorescence and immunohistochemical staining, the areas of fluorescence signal or positive immunohistochemical staining on 3–5 randomly chosen fields (400×)/atrium, five atrial samples in the SR and AF group (total of randomly chosen 16 observations per group), were quantitatively evaluated by Image-Pro Plus 6.0 software (Media Cybernetics). Data were calculated as the percentage of positive-stained area *vs.* total field area. Data are given as the mean±standard deviation (SD). Statistical significance was determined by Student's *t*-test. $p<0.05$ was considered statistically significant.

## 3. Results

### 3.1. In situ gelatinase activity

Gelatinase activity (representing the activity of MMP-2 and MMP-9) in the atrial tissues of AF and SR (i.e., sham control) was evaluated by *in situ* zymography. The green fluorescence caused by the breakdown of DQ-gelatin (reflecting gelatinase activity) was localized at the interstitium of the atria, and showed similar patterns in the AF and SR samples. In atrial tissues with AF, localization of green signal had a thicker fibrillar appearance in the interstitium of myocardium (Fig. 1A) and surrounding the cardiomyocytes (Figs. 1A, C and D). In atrial tissues with SR, there was only a fine network of green signals within the atrial interstitium, and only a faint signal was localized among the cardiomyocytes (Fig. 1B). Quantification of fluorescence measured in the SR and AF atria by *in situ* zymography indicated increased gelatinolytic activity in atrial tissues with AF compared with that in the SR ($p<0.01$) (Fig. 1E).

### 3.2. MMP-2 and MMP-9 activity and protein expression

To further investigate the changes of gelatinase activity in atria with AF, assays of in-gel gelatin zymography on homogenates obtained from atrial tissues with SR and AF were done. The

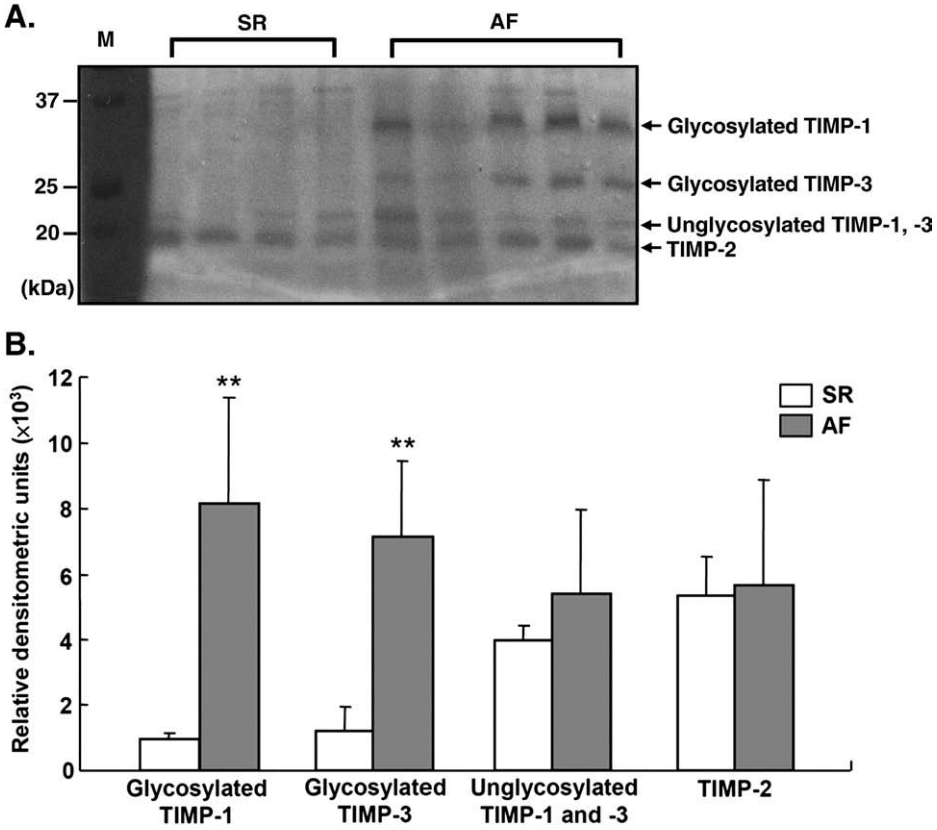


**Fig. 3.** Determination of inhibition of gelatinase activity (i.e., MMP-inhibitory activity of TIMPs) in the atrial homogenates using reverse gelatin zymography analysis. Homogenates (20 μg) from atrial tissues with AF and SR were loaded onto SDS-PAGE gels and processed for reverse gelatin zymography. (A) Representative reverse gelatin zymography is shown. Dark bands are undigested gelatin stained with Coomassie blue, representing the zones of gelatinase inhibition. The migration positions of glycosylated and unglycosylated forms of TIMP-1, TIMP-2 and TIMP-3 are indicated with arrows. Molecular mass markers (M) are indicated on the left. (B) Quantification of reverse gelatin zymography was done. Increased inhibitory activities of glycosylated TIMP-1 and TIMP-3 found in the AF group ($n=9$) reached statistical significance as compared with those in the SR group ($n=6$). Changes in TIMP inhibitory activities in AF samples at 22 kDa (corresponding to the unglycosylated forms of TIMP-1 and TIMP-3) and at 19 kDa (corresponding to TIMP-2) did not reach statistical significance. Each bar indicates mean±SD. $^{**}p<0.01$ *vs.* SR.

representative gelatin zymography in Fig. 2A shows two predominant gelatinase activities migrating at 95 kDa and 68 kDa, corresponding to proMMP-9 (latent form) and MMP-2 (active form), respectively. ProMMP-2 was detected as a band of 72 kDa. A higher molecular weight gelatinolytic band (approximately 220 kDa), corresponding to the dimeric form of proMMP-9 as indicated by previous reports [27–29], was also detected. Confirmation of the migration of latent and active forms of MMP-2 and -9 was carried out using APMA-treated atrial homogenates of AF (Fig. 2A, right panel). The result shows that the gelatinolytic bands of 220 kDa and 95 kDa were mostly converted to the gelatinolytic bands migrated at approximately 85 kDa (corresponding to the activated form of MMP-9) after 60 min of APMA treatment, indicating that gelatinolytic enzymes in atria with AF primarily comprised proMMP-9.

Total zymographic activity of atrial homogenates was quantified using densitometric analysis. Gelatinase activity of MMP-9 (including latent and active forms) in the RAP-induced AF samples significantly increased as compared with those in SR (mean increase = 6.6-fold, $p<0.01$). MMP-2 activity (including latent and active forms) decreased in the AF samples (mean decrease = 2.2-fold, $p<0.05$) (Fig. 2B). The predominant upregulation of MMP-9 was observed in the latent form, but not in the active form (Fig. 2C).

### 3.3. MMP-inhibitory activity of TIMPs

TIMPs are considered to be the important regulators during tissue remodeling because they can inhibit MMPs directly by forming 1:1 enzyme–inhibitor complexes [10,17]. To investigate if TIMP activity was changed in AF, the homogenates of atrial tissues were subjected to reverse zymography for evaluating MMP-inhibitory activity of TIMPs. In Fig. 3A, four bands ranging from 19 kDa to 32 kDa corresponding to gelatinase inhibition by TIMP-1, TIMP-2 and TIMP-3 are depicted. Densitometric analysis of these TIMP activities showed a significant increase ($p<0.01$) at 27 kDa (corresponding to glycosylated TIMP-3) and 32 kDa (corresponding to glycosylated TIMP-1) in AF tissues when compared with both glycosylated TIMPs in the SR tissues (Fig. 3B). MMP-inhibitory activity of unglycosylated forms of TIMP-1 (22 kDa) and TIMP-3 (22 kDa) in the atrial tissues with AF did not show a

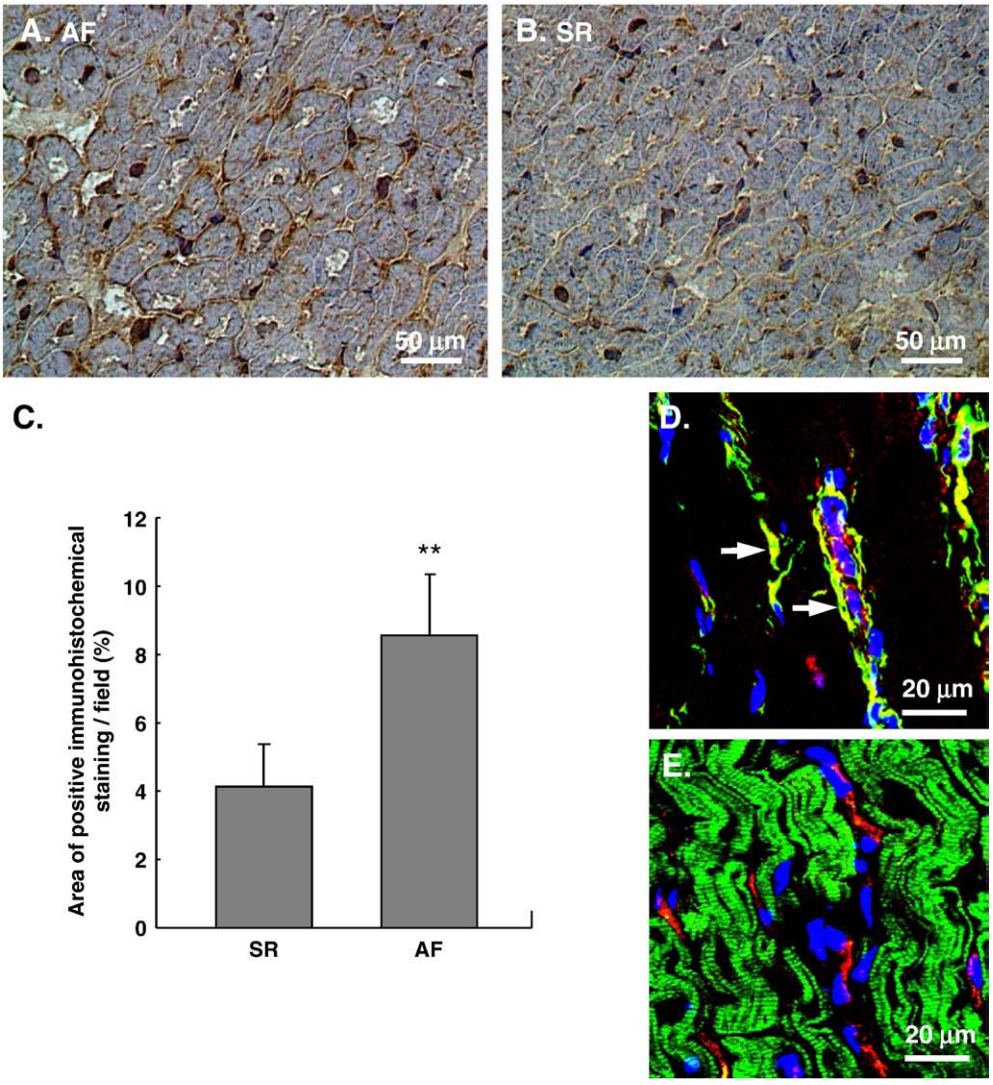


**Fig. 4.** Immunohistochemical and double-immunofluorescence staining for TIMP-1 in AF and SR tissues. Positive immunohistochemical staining for TIMP-1 is brown and the nuclear counterstain is blue. Positive TIMP-1 staining in the atrial interstitium (A and B) is shown. Quantification of the digital images from TIMP-1 immunohistochemical staining was done (C). The increased levels of TIMP-1 staining in the atrial interstitium reached statistical significance in the AF group as compared with that in the SR group. Double-immunofluorescence staining was used to examine TIMP-1 expression (red fluorescence) in the cardiac fibroblasts (vimentin label; green fluorescence; D) and cardiomyocytes (cardiac troponin T label; green fluorescence; E) in AF atria. Nuclei were counterstained with DAPI (blue). The yellowish cells (white arrows) in merged images (D) reveal that TIMP-1 was almost expressed in cardiac fibroblasts, not in cardiomyocytes (E). Each bar in the panel C indicates mean ± SD. $^{**}p<0.01$ *vs.* SR.

statistically significant increase as compared with those in the SR ($p=0.06$). This was also the case for the TIMP-2 activity (19 kDa) ($p=0.1$) (Fig. 3B).

### 3.4. Immunohistochemical staining of TIMP-1 and TIMP-3

Immunohistochemical staining for TIMP-1 and TIMP-3 was performed on atrial tissues obtained from the AF and SR groups. Similar to gelatinase activity, immunoreactive TIMP-1 was mainly localized in the atrial interstitium (Figs. 4A and B). A significant ($p<0.01$) increase in TIMP-1 immunohistochemical staining in the fibrillating atria was found when compared to that in SR atria (Fig. 4C). Moreover, double-immunofluorescence staining for vimentin (specific marker for fibroblasts) and cardiac troponin T (specific marker for cardiomyocytes) also confirmed that the TIMP-1 was almost expressed in the cardiac fibroblasts, not cardiomyocytes, of the AF atria (Figs. 4D and E). Positive immunohistochemical staining for TIMP-3 was also detected in the atrial myocardium (Figs. 5A and B). Compared with the SR group, increased expression of TIMP-3 in the atrial interstitium and cardiomyocytes was observed in AF atria ($p<0.05$) (Fig. 5C). The result of double-immunofluorescence staining showed that TIMP-3 was intensely expressed in cardiac fibroblasts, but mildly expressed in cardiomyocytes of AF tissues (Figs. 5D and E).

### 3.5. mRNA expression of MMPs and TIMPs

To determine whether the changes of gelatinase and MMP-inhibitory activity of TIMPs in the findings stated above correlated with transcriptional levels, the expressed levels of mRNAs encoding MMP-2, MMP-9, TIMP-1, TIMP-2 and TIMP-3 in atrial tissues were assessed by semi-quantitative RT-PCR. Expressed mRNA levels of other important MMPs, including MMP-1 (collagenase), MMP-3 (stromelysin) and MMP-14 (membrane-type-1 MMP; MT1-MMP), were also surveyed. In this experiment, expressed GAPDH mRNA was employed as an internal control. Statistical analysis indicated that there was a 3.9-fold ($p<0.01$) increase in MMP-9 mRNA level in atria with AF as compared with that in SR atria. However, the expressed mRNA levels of MMP-1, MMP-2, and MMP-3 were similar between the

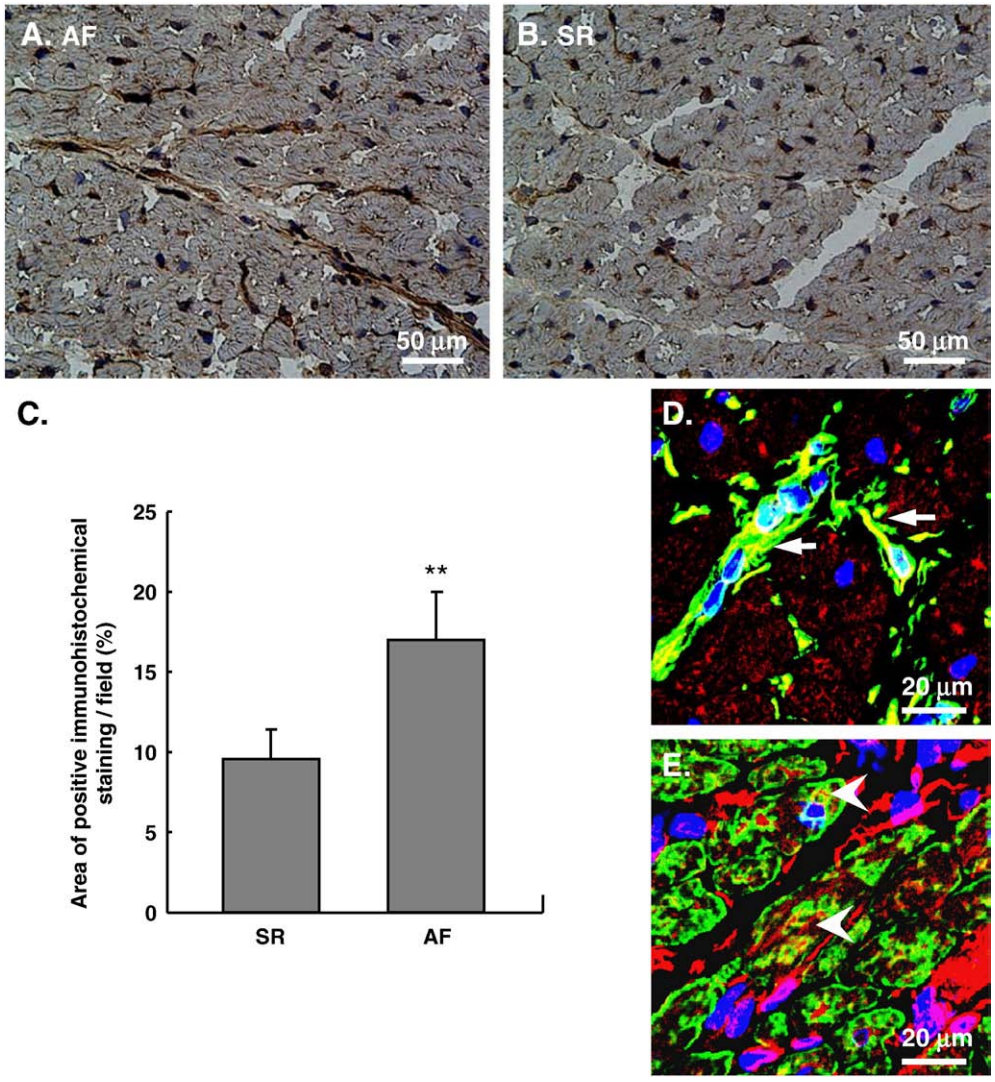


**Fig. 5.** Immunohistochemical and double-immunofluorescence staining for TIMP-3 in AF and SR tissues. Positive immunohistochemical staining for TIMP-3 is brown and the nuclear counterstain is blue. Positive staining for TIMP-3 was confined to the regions of atrial interstitium (A and B). Quantification of the digital images from TIMP-3 immunohistochemical staining was done. Increased TIMP-3 expression reached statistical significance in the AF group as compared with that in the SR group (C). Double-immunofluorescence staining was carried out to examine the localization of TIMP-3 (red fluorescence) in cardiac fibroblasts (vimentin label; green fluorescence; D) and cardiomyocytes (cardiac troponin T label; green fluorescence; E) in AF atria. Nuclei were counterstained with DAPI (blue). In the merged images (D and E), the yellowish cells indicate that TIMP-3 was intensely expressed in cardiac fibroblasts (white arrows), but mildly expressed in cardiomyocytes (white arrowheads). Each bar in the panel C indicates mean ± SD. $^{**}p<0.01$ *vs.* SR.

two groups, while the downregulation of MMP-14 mRNA was found in AF tissues (Fig. 6A). The data not only support the notion that the change of MMP-9 activity is associated with the level of gene expression, but also imply an important role of MMP-9 regulation in the fibrillating atria. Although there was a significant increase in the MMP-inhibitory activity of TIMPs in AF compared with SR tissues (Fig. 3), expressed mRNA levels of TIMP-1, TIMP-2, and TIMP-3 were not significant between the two groups (TIMP-1, $p=0.05$; TIMP-2, $p=0.16$; TIMP-3, $p=0.06$) (Fig. 6B).

### 3.6. Localization of TIMP-1, TIMP-3 and gelatinase activity

We demonstrated a simultaneous increase in gelatinase activity, TIMP-1 and TIMP-3 in the atrial interstitium of RAP-induced AF tissues. The result suggests a more complex interplay between TIMPs and MMPs in atrial remodeling during AF. We considered that the ratio of MMP/TIMP expression may not be sufficient for revealing the relationships between TIMPs and MMPs *in vivo*. To further clarify the interplay between the TIMPs and gelatinase in AF atria, we carried out *in situ* zymography followed by immunofluorescence staining for TIMP-1 or TIMP-3, and then analysis by confocal laser scanning fluorescence microscopy. Fig. 7 reveals a close association between gelatinase activity (green color) and TIMP-1 or TIMP-3 staining (red color), predominantly in the atrial interstitium of AF. TIMP-1 was found to be mostly overlapped with the areas of gelatinase activity (Figs. 7A–C; mean percentage, 82±9%) and appeared not to block its activity. By contrast, TIMP-3 appeared only partial overlap area in the atrial interstitium (Figs. 7D–F; mean percentage, 23±11%). Notably, TIMP-3 distribution also discontinued the gelatinase activity along the peripheral cardiomyocytes at the view of cross and longitudinal sections (Figs. 7G and H), suggesting that TIMP-3 may regulate its activity. These observations indicate that TIMP-1 mostly coexisted with gelatinase activity, and that TIMP-1 and TIMP-3 may have different roles in inhibiting gelatinase activity *in vivo* during atrial remodeling of AF.

### 3.7. TGF-β1 in atria with AF

We previously demonstrated that atrial TGF-β1 mRNA was increased in AF atria compared with that in SR atria [18]. The marked increase of gelatinase activity was also found in the atrial interstitium of AF (Fig. 1). To confirm our supposition that the activation of TGF-β1 in AF atria may be associated with the increased gelatinase activity, immunostaining with antibody against the human TGF-β1 protein was performed to detect protein abundance in the atrial tissues with AF and SR. The single protein chain of TGF-β1 (approximately 15 kDa), corresponding to the activated form of TGF-β1, was observed in the protein homogenates extracted from AF and SR atria (Fig. 8A). On average, densitometric analysis showed that the level of atrial TGF-β1 was significantly increased by 2.7-fold ($p<0.01$) in AF *vs.* SR tissues (Fig. 8B).

## 4. Discussion

We demonstrated the changes in gelatinase activities of MMP-2 and MMP-9 and the MMP-inhibitory activities of TIMP isoforms in the fibrillating atria induced by RAP. Increased *in vivo* gelatinase activity in the atrial interstitium was observed (Fig. 1) and was consequent to the

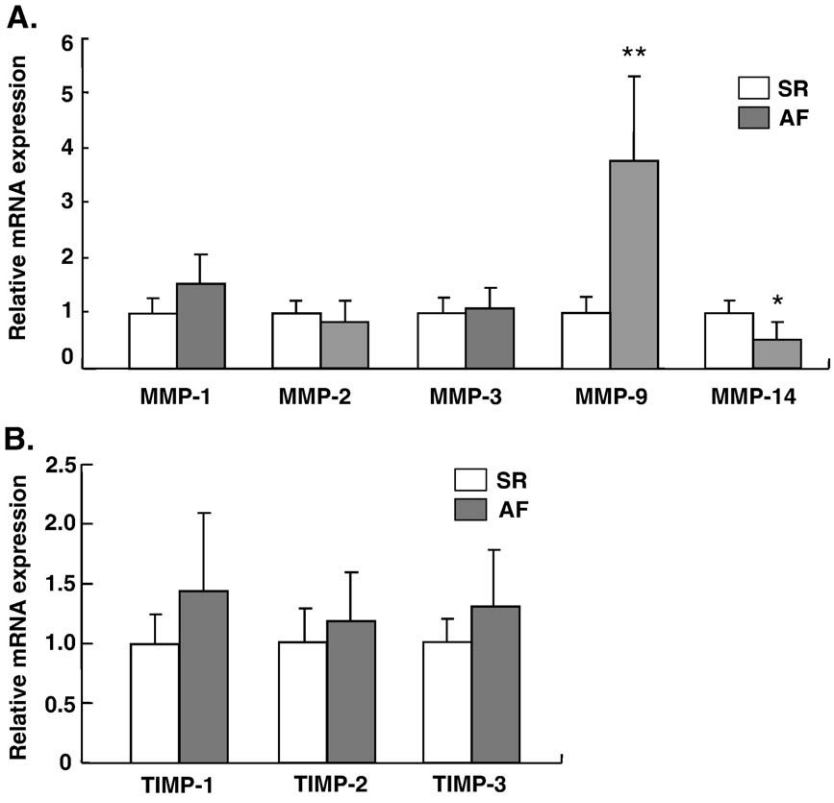


**Fig. 6.** Relative mRNA levels of MMPs and TIMPs in atrial tissues from the AF and SR groups. Expressed mRNA levels of MMP-1 (collagenases), MMP-2 (gelatinase A), MMP-3 (stromelysin), MMP-9 (gelatinase B), MMP-14 (MT1-MMP), TIMP-1, TIMP-2 and TIMP-3 were examined by semi-quantitative RT-PCR. Data were normalized to the level of expressed GAPDH mRNA and expressed relative to the SR group. (A) Relative mRNA levels of MMPs are shown. Upregulation of MMP-9 mRNA was observed in AF samples ($n=9$) as compared with the SR samples ($n=6$) ($p<0.01$). No significant difference in MMP-1, MMP-2 and MMP-3 mRNA levels was found between the AF and SR samples, whereas MMP-14 mRNA was downregulated (mean decrease=1.9-fold, $p<0.05$) in the AF group. (B) Relative mRNA levels of TIMPs are shown. Changes in expressed TIMPs mRNA in AF samples did not reach statistical significance as compared with SR samples. Each bar indicates mean±SD. *$p<0.05$; **$p<0.01$ *vs.* SR.

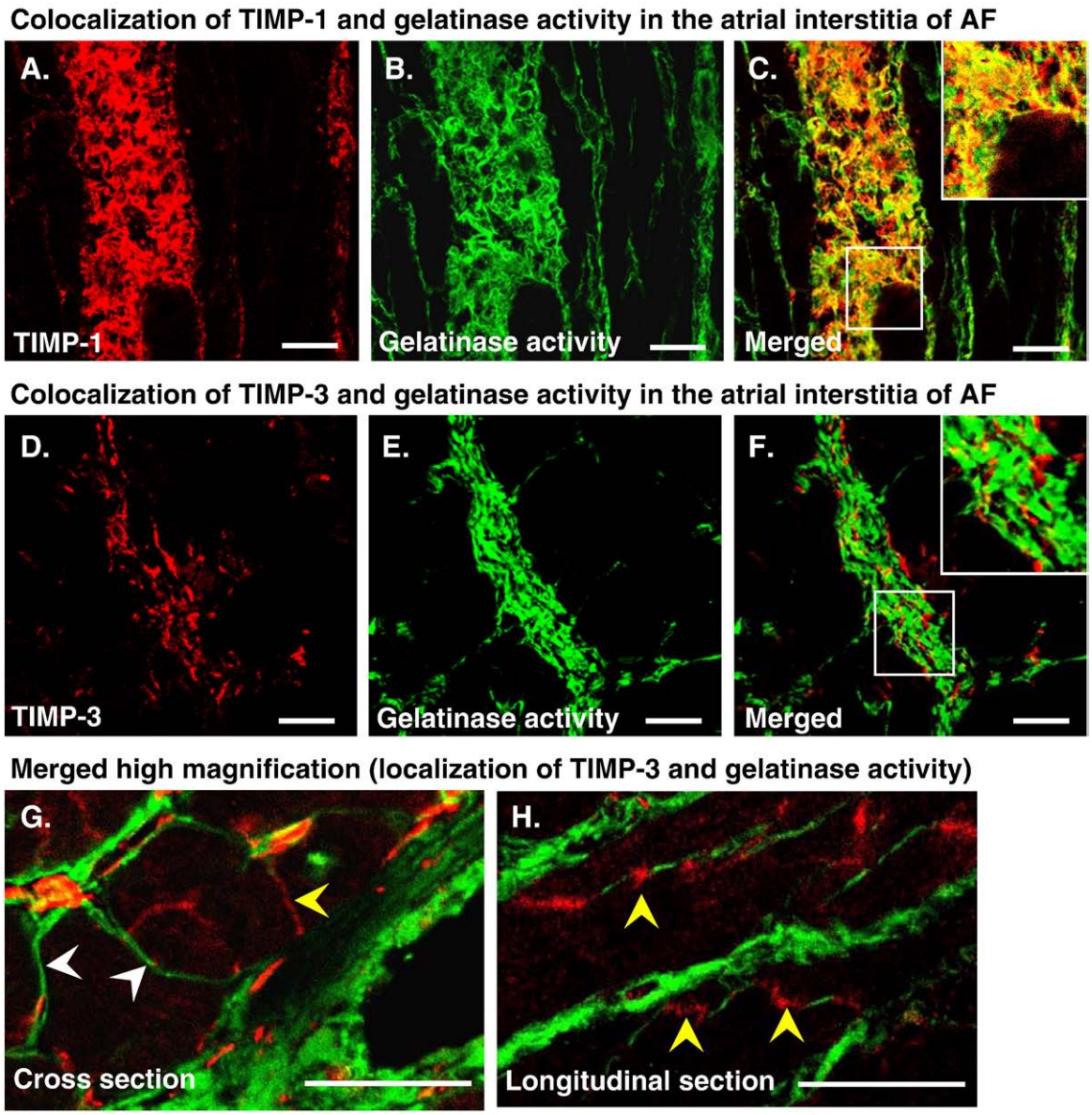


**Fig. 7.** Colocalization of gelatinase activity with TIMP-1 or TIMP-3 in the atrial interstitium of AF by analyzing confocal micrographs of dual fluorescence. Representative confocal micrographs illustrate the localization of TIMP-1 (A) and TIMP-3 (D) (detected with rhodamine red fluorescence) and gelatinase activity (B and E) (detected with green fluorescence yielded by DQ-gelatin degradation) in the interstitium of AF atria. The merged images (C and F) showed the colocalization of TIMP-1 or TIMP-3 with the gelatinase activity by the yellow color. Merged images at higher magnification showed the dual labeling of the TIMP-3 (red color) and gelatinase activity (green color) in the cardiomyocytes in AF tissue (G and H). The presence of TIMP-3 (yellow arrowheads) and gelatinase activity (white arrowheads) along the peripheral cardiomyocytes was clearly depicted at cross section (G). Longitudinal image (H) apparently indicated that the location of gelatinase activity in discrete (arrowheads) was presented by the TIMP-3 instead. Areas of TIMP-1 or TIMP-3 fluorescent stain (red) and its overlap (yellow) with gelatinase activity were quantified. Colocalization analysis indicated that the mean percentage of TIMP-1 colocalized with gelatinase activity was 82 ± 9%, but only 23 ± 11% colocalization of TIMP-3 location was found in the interstitium of AF atria. Values represent mean percentage ± SD. Scale bars, 50 μm.

predominant increase of MMP-9 expression in atria with AF (Fig. 2). Additionally, increased TIMP activities corresponding to glycosylated TIMP-1 and TIMP-3 were also found in AF samples (Fig. 3). The increased TIMP-1 and TIMP-3 localized in the atrial interstitium of AF samples were identified (Figs. 4 and 5). Concordant with our previous work [18–20] that increased interstitial fibrosis and ECM proteins were identified in this AF model, we suggest that the increased activities of gelatinase, glycosylated TIMP-1 and TIMP-3 may contribute to atrial ECM remodeling in RAP-induced AF. Interestingly, via the zymographic and colocalization analyses, additional novel findings in our AF model were that: (i) increased MMP-9 and TIMPs in AF atria were almost exclusively in the pro-form and glycosylated form, respectively (Figs. 2 and 3); and (ii) the high degree of colocalization of TIMP-1 and gelatinase activity were observed in the atrial interstitium of AF (Fig. 7). These data suggest that the post-translational regulation and interaction of proMMP-9 and glycosylated TIMPs may have important roles for ECM remodeling during AF development.

In a rapid pacing-induced atrial failure model in dogs, Hoit et al. [30] found a significantly increased activity of MMP-9 in atrium, but non-significant changes were observed in MMP-2, MMP-3 and MMP-7. Nakano et al. [31] reported that MMP-9 mRNA and protein levels increased in fibrillating human atria, whereas expressed mRNA levels of MMP-2 and TIMP-1 were unchanged. Increased MMP-2 and MMP-9 activities and decreased TIMP-2 expression were associated with AF development in another report [32]. A recent clinical study examined the myocardial collagen content and levels of several MMPs and TIMPs in the four heart chambers and showed that the protein levels of MMP-9 and TIMP-3 were differentially increased in the left atrium

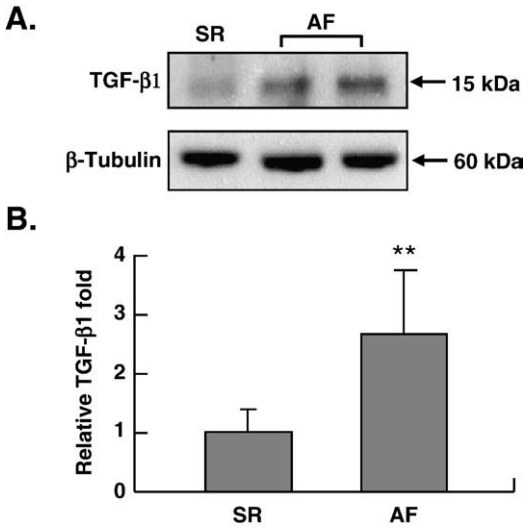


**Fig. 8.** Determination of transforming growth factor-β1 (TGF-β1) protein levels in AF and SR atria. (A) Proteins (20 μg) from the atrial tissues of SR and AF were loaded onto SDS-PAGE gels and followed by Western blot analysis. Lower panel is the loading control staining with anti-β-tubulin antibody. (B) Data were normalized to the level of β-tubulin and expressed relative to the SR group. In the atrial extracts of AF ($n=9$), TGF-β1 (15 kDa) was observed using a rabbit polyclonal anti-human TGF-β1 antibody, and increased by 2.7-fold ($p<0.01$) as compared with those in the SR control ($n=6$). $^{**}p<0.01$ *vs.* SR.

with AF [4]. Among these studies, the most consistent finding was the upregulated MMP-9 during atrial remodeling. In the RAP-induced AF, we estimated mRNA levels of several important MMPs in the atrial tissue, including MMP-2 (gelatinase A), MMP-9 (gelatinase B), MMP-1 (collagenases), MMP-3 (stromelysin), and MMP-14 (MT1-MMP). Consistent with these findings in the animal model and clinical studies, we also found significantly increased atrial MMP-9 in the sustained AF, indicating that increased MMP-9 is a key event in atrial remodeling.

Myocardial fibrosis and ECM remodeling involving increased levels of collagen type I, fibrillin-1 and fibronectin-1 in the atrial interstitium was reported in our RAP-induced AF model [19,20]. Theoretically, an increase in MMP activity should result in a decrease in MMP substrate because MMP activity is the driving force behind degradation of ECM components during tissue remodeling [10,11]; however, our present study indicates a simultaneous increase in gelatinase activity and ECM proteins in RAP-induced AF tissues. This suggests more complex interplay between ECM and MMPs in atrial remodeling during AF. In fact, cardiac fibrosis has been associated not only with increased levels of collagens and alterations in ECM components, but also with increased activity of MMPs, as seen in HF [33,34]. Furthermore, reduced cardiac fibrosis has been associated with decreased activities of MMP-2 and MMP-9 [35]. The apparent paradox may be because MMPs not only directly digest matrix components, but also increase formation of connective tissue by generating bioactive factors from the ECM [3,7,36,37]. For example, it is indicated that MMP-9 can modulate the release or activation of latent TGF-β1 and ECM-bound vascular epithelial growth factor [38,39]. In the RAP-induced AF samples, significantly increased atrial TGF-β1 in active form was found (Fig. 8), suggesting that the increased activity of gelatinase may, in part, facilitate atrial fibrosis by regulating cytokines and matrix-bound growth factors in AF. Data from our previous [18,19,20] and present study point to the critical role of interstitial fibrosis and molecular mechanisms in the atrial remodeling of AF. Given the increased levels of MMP-9 activity, active form of TGF-β1 (a profibrotic cytokine) and ECM proteins in the atrial interstitium of AF, the findings may provide a potential explanation for the increase in the interstitial fibrosis and thereby contribute to AF development.

Marked upregulation of MMP-9 in the RAP-induced AF tissue gave rise to the generation of the pro-form (Fig. 2). As documented for other members of the MMP family, MMP-9 is secreted as a pro-enzyme (proMMP-9) into the extracellular environment, and the activation requires proteolytic processing [40,41]. However, there is considerable evidence that binding of ligand to the proMMP-9, leading to detachment of the propeptide from the active center, increases specific activity by approximately 600-fold compared with that of the unbound proMMP-9, but this is tenfold lower than that of the fully activated form [42]. Accordingly, the marked increase of *in vivo* total gelatinase activity in AF atria in this study was not surprising, even though the major species of MMP-9 was the pro-form (Fig. 2C). On the other hand, fewer amounts of fully activated MMP-9 in AF samples may result from the increased protein of TIMP-1 (Fig. 3), which can inhibit the activation of proMMP-9 by forming a complex with proMMP-9 [43]. Reduced expression of MMP-14 (Fig. 6A) may also result in a reducing cascade of zymogen activation in AF atria [41]. Additionally, proMMP-9 can form a high-affinity complex on the cell surface, indicating that the cell surface association of proMMP-9 is not directly linked to the activation process, but rather plays a role in the microenvironment, where proMMP-9 can be poised for activation by specific proteinases [44]. Gelatinase activity surrounding the cardiomyocytes in AF atria was apparent in this study (Figs. 1C and D). Taken together, we suggest that the remarkable increase in proMMP-9 seen in AF atria may be confined to the ECM, and thus serve as an extracellular pro-enzyme pool for local and rapid activation and mobilization of MMP-9.

AF atria contained abundant glycosylated TIMP-1 and TIMP-3, but neither mRNAs showed a significant increase in expression (Fig. 6B), suggesting a role of post-translational regulation of TIMPs in the fibrillating atria. Even though glycosylation is not always necessary for TIMP function, it plays a part in correct folding of the nascent protein, transport of the molecule to the cell surface, and enhanced stability of the protein [45]. Accordingly, glycosylation of TIMP-1 and TIMP-3 may provide protection against proteolytic degradation, and prolong their half-life in AF. Furthermore, to address the intriguing observation that net gelatinase activity and its inhibitors, TIMP-1 and TIMP-3, were simultaneously increased in AF tissues, their *in vivo* relationships were investigated by colocalization analysis. A high degree of colocalization of TIMP-1 and gelatinase activity was found (Fig. 7C), revealing that TIMP-1 coexists with gelatinase activity, and may allow formation of a complex with proMMP-9 in AF atria. We speculate that the N-terminal domain (catalytic region) of proMMP-9 may retain activity since TIMP-1 binding to proMMP-9 is reversible and through the C-terminal domain of each molecule [46,47]. A recent study showed that aberrancy glycosylated TIMP-1 has a weaker association with proMMP-9 than normal TIMP-1 [48]. Accordingly, a weakened association between glycosylated TIMP-1 and proMMP-9 in AF tissues was suggested for the observation. By contrast, less colocalization of TIMP-3 and gelatinase activity in the atrial interstitium was found (Fig. 7F). Of remarkable interest, the TIMP-3 location was observed instead of the discrete gelatinase activity on the cardiomyocyte surface (Figs. 7G and H), implying that TIMP-3 may regulate the activity of gelatinase in the AF atria. For the observation, there is also the possibility that the gelatinase may have a well-separated localization from TIMP-3 in the atrial myocardium of AF, thus the observed gelatinase activity would be unrelated to the MMP-inhibitory activity of TIMP-3. The reason for the differential performances between TIMP-1 and TIMP-3 is not clear, but the unique properties of TIMP-3 (e.g., inhibitory capacity of TIMP-3 is enhanced within ECM environment, and TIMP-3 interacts with both the N- and C-terminal domains of gelatinases) [49] might be reasoned. In addition to the MMP-inhibitory activity of these TIMPs, the complexes of TIMPs/proMMPs have been demonstrated to regulate proMMPs activation and increase the inhibition rate of activated MMPs [43,50,51], thus regulating degradation of the ECM. These studies strongly support our suggestion

that the increased TIMP-1, TIMP-3 and their complexes with proMMP-9 may facilitate myocardial fibrosis by increasing the inhibition of MMPs in AF atria.

In summary, we clearly showed a striking increase in gelatinase activity in AF. This may be associated with the activation of TGF-β1 and contribute to ECM remodeling. Additionally, by post-translational stabilization of TIMP-1 and TIMP-3 via glycosylation, the increase in MMP-inhibitory activity of TIMPs in the fibrillating atria may provide regulation of proMMP-9 activation and inhibition of the activated MMPs through their inhibitory ability or complexes with proMMP-9. The identification of changes in certain species of MMP and TIMP, as well as their *in vivo* interplay in the RAP-induced AF model, may improve understanding of the pathogenesis of atrial remodeling during AF development.

## Acknowledgments

This work was supported by the grant of NSC 95-2313-B-009-002-MY3 from the National Science Council, and the grant of ATU Programs from the Ministry of Education, Taiwan.

## References

[1] Allessie M, Ausma J, Schotten U. Electrical, contractile and structural remodeling during atrial fibrillation. Cardiovasc Res 2002;54:230–46.
[2] Nattel S, Shiroshita-Takeshita A, Brundel BJ, Rivard L. Mechanisms of atrial fibrillation: lessons from animal models. Prog Cardiovasc Dis 2005;48:9–28.
[3] Lin CS, Pan CH. Regulatory mechanisms of atrial fibrotic remodeling in atrial fibrillation. Cell Mol Life Sci 2008;65:1489–508.
[4] Mukherjee R, Herron AR, Lowry AS, Stroud RE, Stroud MR, Wharton JM, et al. Selective induction of matrix metalloproteinases and tissue inhibitor of metalloproteinases in atrial and ventricular myocardium in patients with atrial fibrillation. Am J Cardiol 2006;97:532–7.
[5] Thijssen VL, Ausma J, Borgers M. Structural remodelling during chronic atrial fibrillation: act of programmed cell survival. Cardiovasc Res 2001;52:14–24.
[6] Singh RB, Dandekar SP, Elimban V, Gupta SK, Dhalla NS. Role of proteases in the pathophysiology of cardiac disease. Mol Cell Biochem 2004;263:241–56.
[7] Mott JD, Werb Z. Regulation of matrix biology by matrix metalloproteinases. Curr Opin Cell Biol 2004;16:558–64.
[8] Parikka V, Vaananen A, Risteli J, Salo T, Sorsa T, Vaananen HK, et al. Human mesenchymal stem cell derived osteoblasts degrade organic bone matrix in vitro by matrix metalloproteinases. Matrix Biol 2005;24:438–47.
[9] Zhang X, Nothnick WB. The role and regulation of the uterine matrix metalloproteinase system in menstruating and non-menstruating species. Front Biosci 2005;10:353–66.
[10] Nagase H, Visse R, Murphy G. Structure and function of matrix metalloproteinases and TIMPs. Cardiovasc Res 2006;69:562–73.
[11] Page-McCaw A, Ewald AJ, Werb Z. Matrix metalloproteinases and the regulation of tissue remodelling. Nat Rev Mol Cell Biol 2007;8:221–33.
[12] Creemers EE, Cleutjens JP, Smits JF, Daemen MJ. Matrix metalloproteinase inhibition after myocardial infarction: a new approach to prevent heart failure? Circ Res 2001;89:201–10.
[13] Spinale FG. Matrix metalloproteinases: regulation and dysregulation in the failing heart. Circ Res 2002;90:520–30.
[14] Newby AC. Dual role of matrix metalloproteinases (matrixins) in intimal thickening and atherosclerotic plaque rupture. Physiol Rev 2005;85:1–31.
[15] Coker ML, Doscher MA, Thomas CV, Galis ZS, Spinale FG. Matrix metalloproteinase synthesis and expression in isolated LV myocyte preparations. Am J Physiol 1999;277:H777–787.
[16] Mukherjee R, Mingoia JT, Bruce JA, Austin JS, Stroud RE, Escobar GP, et al. Selective spatiotemporal induction of matrix metalloproteinase-2 and matrix metalloproteinase-9 transcription after myocardial infarction. Am J Physiol: Heart Circ Physiol 2006;291:H2216–2228.
[17] Gomez DE, Alonso DF, Yoshiji H, Thorgeirsson UP. Tissue inhibitors of metalloproteinases: structure, regulation and biological functions. Eur J Cell Biol 1997;74:111–22.
[18] Chen CL, Lin JL, Lai LP, Pan CH, Huang SK, Lin CS. Altered expression of FHL1, CARP, TSC-22 and P311 provide insights into complex transcriptional regulation in pacing-induced atrial fibrillation. Biochim Biophys Acta 2007;1772:317–29.
[19] Lin CS, Lai LP, Lin JL, Sun YL, Hsu CW, Chen CL, et al. Increased expression of extracellular matrix proteins in rapid atrial pacing-induced atrial fibrillation. Heart Rhythm 2007;4:938–49.
[20] Pan CH, Lin JL, Lai LP, Chen CL, Stephen Huang SK, Lin CS. Downregulation of angiotensin converting enzyme II is associated with pacing-induced sustained atrial fibrillation. FEBS Lett 2007;581:526–34.
[21] Lin JL, Lai LP, Lin CS, Du CC, Wu TJ, Chen SP, et al. Electrophysiological mapping and histological examinations of the swine atrium with sustained (> or = 24 h) atrial fibrillation: a suitable animal model for studying human atrial fibrillation. Cardiology 2003;99:78–84.
[22] Yan SJ, Blomme EA. In situ zymography: a molecular pathology technique to localize endogenous protease activity in tissue sections. Vet Pathol 2003;40:227–36.
[23] Turini P, Kurooka S, Steer M, Corbascio AN, Singer TP. The action of phenylmethylsulfonyl fluoride on human acetylcholinesterase, chymotyrpsin and trypsin. J Pharmacol Exp Ther 1969;167:98–104.
[24] Stawowy P, Margeta C, Kallisch H, Seidah NG, Chretien M, Fleck E, et al. Regulation of matrix metalloproteinase MT1-MMP/MMP-2 in cardiac fibroblasts by TGF-beta1 involves furin-convertase. Cardiovasc Res 2004;63:87–97.
[25] Stetler-Stevenson WG, Krutzsch HC, Wacher MP, Margulies IM, Liotta LA. The activation of human type IV collagenase proenzyme. Sequence identification of the major conversion product following organomercurial activation. J Biol Chem 1989;264:1353–6.
[26] Oliver GW, Leferson JD, Stetler-Stevenson WG, Kleiner DE. Quantitative reverse zymography: analysis of picogram amounts of metalloproteinase inhibitors using gelatinase A and B reverse zymograms. Anal Biochem 1997;244:161–6.
[27] Goldberg GI, Strongin A, Collier IE, Genrich LT, Marmer BL. Interaction of 92-kDa type IV collagenase with the tissue inhibitor of metalloproteinases prevents dimerization, complex formation with interstitial collagenase, and activation of the proenzyme with stromelysin. J Biol Chem 1992;267:4583–6.
[28] Kjeldsen L, Johnsen AH, Sengelov H, Borregaard N. Isolation and primary structure of NGAL, a novel protein associated with human neutrophil gelatinase. J Biol Chem 1993;268:10425–32.
[29] Olson MW, Bernardo MM, Pietila M, Gervasi DC, Toth M, Kotra LP, et al. Characterization of the monomeric and dimeric forms of latent and active matrix metalloproteinase-9. Differential rates for activation by stromelysin 1. J Biol Chem 2000;275:2661–8.
[30] Hoit BD, Takeishi Y, Cox MJ, Gabel M, Kirkpatrick D, Walsh RA, et al. Remodeling of the left atrium in pacing-induced atrial cardiomyopathy. Mol Cell Biochem 2002;238:145–50.
[31] Nakano Y, Niida S, Dote K, Takenaka S, Hirao H, Miura F, et al. Matrix metalloproteinase-9 contributes to human atrial remodeling during atrial fibrillation. J Am Coll Cardiol 2004;43:818–25.
[32] Xu J, Cui G, Esmailian F, Plunkett M, Marelli D, Ardehali A, et al. Atrial extracellular matrix remodeling and the maintenance of atrial fibrillation. Circulation 2004;109:363–8.
[33] Peterson JT, Li H, Dillon L, Bryant JW. Evolution of matrix metalloprotease and tissue inhibitor expression during heart failure progression in the infarcted rat. Cardiovasc Res 2000;46:307–15.
[34] Boixel C, Fontaine V, Rucker-Martin C, Milliez P, Louedec L, Michel JB, et al. Fibrosis of the left atria during progression of heart failure is associated with increased matrix metalloproteinases in the rat. J Am Coll Cardiol 2003;42:336–44.
[35] Meiners S, Hocher B, Weller A, Laule M, Stangl V, Guenther C, et al. Down-regulation of matrix metalloproteinases and collagens and suppression of cardiac fibrosis by inhibition of the proteasome. Hypertension 2004;44:471–7.
[36] Maquart FX, Pickart L, Laurent M, Gillery P, Monboisse JC, Borel JP. Stimulation of collagen synthesis in fibroblast cultures by the tripeptide–copper complex glycyl-L-histidyl-L-lysine-$Cu^{2+}$. FEBS Lett 1988;238:343–6.
[37] Wegrowski Y, Maquart FX, Borel JP. Stimulation of sulfated glycosaminoglycan synthesis by the tripeptide–copper complex glycyl-L-histidyl-L-lysine-$Cu^{2+}$. Life Sci 1992;51:1049–56.
[38] Engsig MT, Chen QJ, Vu TH, Pedersen AC, Therkidsen B, Lund LR, et al. Matrix metalloproteinase 9 and vascular endothelial growth factor are essential for osteoclast recruitment into developing long bones. J Cell Biol 2000;151:879–89.
[39] Yu Q, Stamenkovic I. Cell surface-localized matrix metalloproteinase-9 proteolytically activates TGF-beta and promotes tumor invasion and angiogenesis. Genes Dev 2000;14:163–76.
[40] Nagase H, Woessner Jr JF. Matrix metalloproteinases. J Biol Chem 1999;274:21491–4.
[41] Murphy G, Stanton H, Cowell S, Butler G, Knauper V, Atkinson S, et al. Mechanisms for pro matrix metalloproteinase activation. APMIS 1999;107:38–44.
[42] Bannikov GA, Karelina TV, Collier IE, Marmer BL, Goldberg GI. Substrate binding of gelatinase B induces its enzymatic activity in the presence of intact propeptide. J Biol Chem 2002;277:16022–7.
[43] Ogata Y, Itoh Y, Nagase H. Steps involved in activation of the pro-matrix metalloproteinase 9 (progelatinase B)-tissue inhibitor of metalloproteinases-1 complex by 4-aminophenylmercuric acetate and proteinases. J Biol Chem 1995;270:18506–11.
[44] Olson MW, Toth M, Gervasi DC, Sado Y, Ninomiya Y, Fridman R. High affinity binding of latent matrix metalloproteinase-9 to the alpha2(IV) chain of collagen IV. J Biol Chem 1998;273:10672–81.
[45] Caterina NC, Windsor LJ, Bodden MK, Yermovsky AE, Taylor KB, Birkedal-Hansen H, et al. Glycosylation and NH2-terminal domain mutants of the tissue inhibitor of metalloproteinases-1 (TIMP-1). Biochim Biophys Acta 1998;1388:21–34.
[46] Goldberg GI, Strongin A, Collier IE, Genrich LT, Marmer BL. Interaction of 92-kDa type IV collagenase with the tissue inhibitor of metalloproteinases prevents dimerization, complex formation with interstitial collagenase, and activation of the proenzyme with stromelysin. J Biol Chem 1992;267:4583–91.
[47] Han YP, Nien YD, Garner WL. Tumor necrosis factor-alpha-induced proteolytic activation of pro-matrix metalloproteinase-9 by human skin is controlled by down-regulating tissue inhibitor of metalloproteinase-1 and mediated by tissue-associated chymotrypsin-like proteinase. J Biol Chem 2002;277:27319–27.
[48] Kim YS, Hwang SY, Kang HY, Sohn H, Oh S, Kim JY, et al. Functional proteomics study reveals that *N*-acetylglucosaminyltransferase V reinforces the invasive/

metastatic potential of colon cancer through aberrant glycosylation on tissue inhibitor of metalloproteinase. Mol Cell Proteomics 2008;7:1–14.
[49] Butler GS, Apte SS, Willenbrock F, Murphy G. Human tissue inhibitor of metalloproteinases 3 interacts with both the N- and C-terminal domains of gelatinases A and B. Regulation by polyanions. J Biol Chem 1999;274:10846–51.
[50] Hayakawa T, Yamashita K, Ohuchi E, Shinagawa A. Cell growth-promoting activity of tissue inhibitor of metalloproteinases-2 (TIMP-2). J Cell Sci 1994;107:2373–9.
[51] Kolkenbrock H, Orgel D, Hecker-Kia A, Noack W, Ulbrich N. The complex between a tissue inhibitor of metalloproteinases (TIMP-2) and 72-kDa progelatinase is a metalloproteinase inhibitor. Eur J Biochem 1991;198:775–81.